Alteration of retinal rod outer segment membrane fluidity in a rat model of Smith-Lemli-Opitz syndrome

Kathleen Boesze-Battaglia,[*] Monika Damek-Poprawa,[*] Drake C. Mitchell,[†] Laura Greeley,[†] Richard S. Brush,[§,††] Robert E. Anderson,[§,,††] Michael J. Richards,[§§] and Steven J. Fliesler[1,§§,***]**

From the Department of Biochemistry,[*] School of Dental Medicine, University of Pennsylvania, Philadelphia, PA 19104; the Laboratory of Membrane Biochemistry and Biophysics,[†] National Institute on Alcohol Abuse and Alcoholism, National Institutes of Health, Bethesda, MD 20892; the Departments of Ophthalmology[§] and Cell Biology,[**] University of Oklahoma Health Sciences Center, and Dean McGee Eye Institute,[††] Oklahoma City, OK 73104; and the Departments of Ophthalmology[§§] (Saint Louis University Eye Institute) and Pharmacological & Physiological Science,[***] Saint Louis University School of Medicine, St. Louis, MO 63104

Abstract Smith-Lemli-Opitz syndrome (SLOS) is caused by an inherited defect in the last step in cholesterol (Chol) biosynthesis, leading to abnormal accumulation of 7-dehydrocholesterol and decreased Chol levels. Progressive retinal degeneration occurs in an animal model of SLOS, induced by treating rats with AY9944, a selective inhibitor of the enzyme affected in SLOS. Here we evaluated alterations in the biochemical and physical properties of retinal rod outer segment (ROS) membranes in this animal model. At 1 month of AY9944 treatment, there were modest alterations in fatty acid composition, but no significant differences in *cis*-parinaric acid (*c*PA) spectroscopic parameters in ROS membranes from treated versus control rats. However, at 3 months, ROS docosahexaenoic acid (DHA) content was dramatically reduced, and *c*PA fluorescence anisotropy values were decreased, relative to controls. Also, 1,6-diphenyl-1,3,5-hexatriene exhibited decreased rotational motion and increased orientational order in ROS membranes from 3 month-old AY9944-treated rats, relative to controls. No significant changes in protein:lipid ratios were observed; however, rhodopsin regenerability was compromised by 3 months of treatment. These findings are consistent with reduced ROS membrane fluidity in the SLOS rat model, relative to controls, primarily due to the dramatic reduction in membrane DHA levels, rather than altered sterol composition.—Boesze-Battaglia, K., M. Damek-Poprawa, D. C. Mitchell, L. Greeley, R. S. Brush, R. E. Anderson, M. J. Richards, and S. J. Fliesler. **Alteration of retinal rod outer segment membrane fluidity in a rat model of Smith-Lemli-Opitz syndrome. *J. Lipid Res.* 2008.** 49: **1488–1499.**

Supplementary key words fluorescence polarization • *cis*-parinaric acid • diphenylhexatriene • fatty acid • retina • AY9944

Inborn errors of cholesterol (Chol) biosynthesis comprise a constellation of typically severe, often lethal, human hereditary diseases having distinct genetic, biochemical, and phenotypic characteristics, yet sharing the common feature of abnormally low Chol levels in all tissues (as reviewed in Refs. 1, 2). The Smith-Lemli-Opitz syndrome (SLOS) is an autosomal recessive disorder with associated multiple congenital anomalies (3), and is caused by an enzymatic defect in the last step of the Chol biosynthetic pathway (as reviewed in Ref. 4). The typical biochemical signature of this syndrome is elevated levels of 7-dehydrocholesterol (7DHC) together with reduced levels of Chol in blood and other tissues, relative to the levels found in normal individuals. These abnormalities are the consequence of mutations in the *DHCR7* gene, which encodes the enzyme DHCR7 (3β-hydroxy-sterol-Δ^7-reductase; EC 1.3.1.21) (4); the mutant enzyme inefficiently catalyzes the conversion of 7DHC to Chol. The central nervous system, in particular, is often profoundly affected in SLOS patients, as manifested by moderate to severe mental retardation and autism (1, 2, 4). Retinal dysfunction also appears to be an associated feature of the disease, evidenced by rod photoreceptor electrophysiological defects (5).

A pharmacologically induced animal model of SLOS has been developed by treating rats with AY9944, a selective inhibitor of DHCR7 (6–8). We previously described a progressive (age-dependent) retinal degeneration in such an

This study was supported by United States Public Health System, National Institutes of Health Grants EY-007361 (S.J.F.), EY-00871 (R.E.A.), EY-04149 (R.E.A.), EY-10420 (K.B-B.), EY-12190 (R.E.A.), and RR-17703 (R.E.A); the Foundation Fighting Blindness (R.E.A.); and unrestricted departmental grants from Research to Prevent Blindness (S.J.F. and R.E.A.). K.B-B. is the recipient of an E. Matilda Ziegler Vision Award. S.J.F is the recipient of a Research to Prevent Blindness Senior Scientific Investigator Award.

Manuscript received 16 January 2008 and in revised form 10 March 2008.

Published, JLR Papers in Press, March 14, 2008.
DOI 10.1194/jlr.M800031-JLR200

Abbreviations: 7DHC, 7-dehydrochosterol; BRD, Brownian rotational diffusion; Chol, cholesterol; *c*PA, *cis*-parinaric acid; DHA, docosahexaenoic acid; DPH, 1,6-diphenyl-1,3,5-hexatriene; mAb, monoclonal antibody; ROS, rod outer segment; SLOS, Smith-Lemli-Opitz syndrome.

[1] To whom correspondence should be addressed.
e-mail: fliesler@slu.edu

animal model, with associated biochemical, histological, and electrophysiological abnormalities involving both rod and cone photoreceptors (7, 8). By 1 postnatal month, although retinal histology and electrophysiological competence in AY9944-treated rats appeared grossly unaffected, the mole ratio of 7DHC:Chol in the retina was nearly 4:1, whereas the normal rat retina contains virtually no 7DHC (7). In striking contrast, by 3 postnatal months, retinas of AY9944-treated rats had 7DHC:Chol mole ratios typically >5:1, and exhibited concomitant histological degeneration along with rod and cone electrophysiological abnormalities (8). Subsequently, in the course of lipidomic analysis of whole retinas from age-matched control and AY9944-treated rats, we recently documented a marked decline in docosahexaenoic acid (DHA; 22:6n3) content of the major retinal glycerophospholipid molecular species in the SLOS rat model, relative to controls (9). However, under the conditions employed, the DHA levels in serum and liver were not lower than those found in normal controls, indicating that there was no generalized, systemic n3 fatty acid deficiency.

In the present study, we performed subcellular fractionation of retinas from AY9944-treated and age-matched control rats to obtain purified rod outer segment (ROS) membranes, and then analyzed their fatty acid content and membrane fluidity, the latter by fluorescence spectroscopy using two independent, naturally fluorescent probes: *cis*-parinaric acid (*c*PA; 9*Z*,11*E*,13*E*,15*Z*-octadecatetraenoic acid) and 1,6-diphenyl-1,3,5-hexatriene (DPH). These linear fluorescent fatty acid probes are useful in detecting and quantifying gel–fluid heterogeneity in lipid bilayers (as reviewed in Ref. 10). *c*PA is a fluorescent n3 PUFA that serves as one of the closest structural analogs to endogenous membrane lipids. This probe is routinely used to evaluate molecular packing density and as a peroxidation indicator (11). DPH, one of the most commonly used fluorescent membrane probes, is an extremely hydrophobic, symmetrical, rod-like *trans*-polyene that penetrates into the hydrophobic core of the bilayer, where its fluorescence intensity is over 10,000 times higher than in water (as reviewed in Ref. 12). It is widely employed for assessing membrane phase and fluidity using both steady-state and time-resolved fluorescence spectroscopy. Time-resolved measurements enable discrimination between simultaneous changes in probe lifetime, probe motion, and angular distribution in the membrane hydrophobic core. DPH fluorescence lifetime is exquisitely sensitive to changes in local dielectric properties, making it ideal for assessing changes in transient water penetration into the membrane (13), and time-resolved fluorescence depolarization of DPH can provide detailed information about membrane orientational order and dynamics (13, 14).

Here we show that the fluidity of ROS membranes is significantly reduced in the SLOS rat model, relative to controls, concomitant with the timing of retinal degeneration in that model. We provide correlative evidence and a rationale that supports the conclusion that the marked decrease in membrane lipid unsaturation, largely due to losses in DHA, rather than to alterations in the sterol profile, accounts for the altered membrane fluidity. Furthermore, the efficiency of rhodopsin regeneration is compromised in the SLOS rat model, relative to controls, even in the presence of excess chromophore (11-*cis* retinaldehyde). The results are discussed within the context of how such changes may impact the efficiency of phototransduction in the rod cell and the overall electrophysiological competence of the retina, with relevance to visual defects observed in the SLOS rat model as well as in SLOS patients.

EXPERIMENTAL PROCEDURES

Materials

AY9944 (*trans*-1,4-*bis*(2-chlorobenzylamino-methyl)cyclohexanedihydrochloride) was custom synthesized, and matched the spectroscopic and physical properties of an authentic sample of AY9944 (kindly provided by Wyeth-Ayerst Laboratories, Monmouth, NJ). All organic solvents were of HPLC grade, and used as purchased from Fisher Scientific (Pittsburgh, PA). Fatty acid standards were used as purchased from Nu-Chek Prep, Inc. (Elysian, MN). Sterol standards were obtained from Steraloids, Inc. (Newport, RI); 7DHC was periodically recrystallized from methanol-water and its purity verified by HPLC prior to use. Anti-opsin monoclonal antibody (mAb 4D2) was a generous gift from Dr. Robert Molday (University of British Columbia, Vancouver, BC). HRP-conjugated secondary antibodies were obtained from Amersham Biosciences (Piscataway, NJ). Protein molecular weight standards were obtained from BioRad (Hercules, CA). 11-*cis* Retinal was kindly provided by Dr. Rosalie Crouch (Medical College of South Carolina, Charleston, SC). *c*PA (9*Z*,11*E*,13*E*,15*Z*-octatetradecanoic acid) and DPH were purchased from Molecular Probes/Invitrogen (Carlsbad, CA). Unless otherwise specified, all other reagents were used as purchased from Sigma/Aldrich (St. Louis, MO). Alzet® osmotic pumps (Model 2ML4) were purchased from Durect Corporation (Cupertino, CA).

Animals

All procedures involving animals were approved by the Saint Louis University IACUC and conformed to the National Institutes of Health's *Guide for the Care and Use of Laboratory Animals* and the Association for Research in Vision and Ophthalmology's *Statement for the Use of Animals in Ophthalmic and Visual Research*. Adult female Sprague-Dawley rats (pregnant, 6 days sperm-positive) were obtained from Harlan (Indianapolis, IN). Rats were fed a standard rat chow (Purina Mills TestDiet, Richmond, IN) and were provided continuous access to water, ad libitum. In-house analysis confirmed that the chow was essentially Chol-free (data not shown). Rats were treated with AY9944 as previously described (8, 15). In brief, pregnant rats were implanted subcutaneously with Alzet® osmotic pumps containing AY9944 (in PBS solution, 1.5 mg/ml), so as to provide continuous delivery of AY9944 at a uniform rate (0.37 mg/kg/day, at 2.5 μl/h), beginning on gestational day 7 and continuing through the second postnatal week. Control dams received the same food and water ad libitum, but received no other treatment. Starting on postnatal day 1, the progeny of AY9944-treated dams were injected subcutaneously on alternating days, three times per week, with AY9944 (30 mg/kg, in PBS); treatment continued over a 3 month time course.

ROS membrane preparation

ROS membranes were prepared from dark-adapted rat retinas (four pooled retinas per preparation) by discontinuous sucrose

density ultracentrifugation, essentially as described previously (16), with the modifications detailed in (17). All procedures were performed in darkness or under dim red light (15W incandescent light bulbs with Wratten #2 filters; Eastman Kodak, Rochester, NY). Membranes were washed twice with ice-cold Tris-Mg buffer (10 mM Tris-acetate, pH 7.4, containing 5 mM $MgCl_2$) containing diethylene triamine pentaacetic acid (0.1 mM), butylated hydroxytoluene (0.01 mg/ml), and $SnCl_2$ (0.01 mg/ml) to retard lipid peroxidation, by ultracentrifugation (Beckman TLA-45 rotor, 10 min at 100,000 *g*, 4°C; Beckman Optima-TL centrifuge; Beckman Instruments, Palo Alto, CA). The membrane pellets were resuspended by brief probe sonication in ice-chilled HEPES-buffered saline (10 mM HEPES, pH 7.4, containing 100 mM NaCl) and flash frozen (in capped microcentrifuge tubes, flushed with argon) in liquid nitrogen, then wrapped in aluminum foil and stored in darkness at −80°C until used for analysis.

Rhodopsin regeneration studies

ROS membranes (resuspended in HEPES-buffered saline containing 10 mM hydroxylamine hydrochloride) were bleached by continuous illumination using a light source equipped with an orange filter, as previously described (18). Routinely greater than 90% of the total rhodopsin was bleached under these conditions. In all experiments, the duration of bleaching was adjusted such that the same total amount of rhodopsin was bleached in the membranes being compared. The bleached membranes were washed twice in 10 mM HEPES, pH 7.4 and centrifuged, and the supernatant containing the excess hydroxylamine was discarded. Rhodopsin was regenerated from the apoprotein opsin by the addition of a 2–3-fold molar excess of 11-*cis* retinal, prepared in ethanol, such that the final ethanol concentration was 0.5% (v/v). The samples were incubated in the dark at 37°C, and aliquots were removed for spectrophotometric analysis at 2.5, 4, and 24 h. The extent of rhodopsin regeneration was measured spectrophotometrically as an increase in absorbance at 500 nm, using a Perkin-Elmer Lambda 25 UV/Vis spectrophotometer (PerkinElmer Life and Analytical Sciences, Inc.; Waltham, MA) equipped with a temperature-controlled microcuvette holder. The percent rhodopsin regenerated was calculated based on the amount of rhodopsin bleached in each sample analyzed.

SDS-PAGE and immunoblotting

Detergent-solubilized ROS membranes from control and AY9944-treated rats were prepared as described previously (19); proteins were separated on 12% SDS-PAGE under reducing conditions and immunoblotted essentially per the method of Towbin, Staehelin, and Gordon (20), normalized to total lipid phosphorus load (1 mg) per lane. Western blots were probed with a 1:1,000 dilution of mouse anti-opsin mAb 4D2, followed by a 1:1,000 dilution of sheep anti-mouse, HRP-conjugated secondary antibody. Immunoblots were visualized using an enhanced chemifluorescence detection system (Amersham Biosciences; Arlington Heights, IL), which allegedly (per the manufacturer) provides better signal linearity than some commonly used chemiluminescent detection systems. Digital analysis of blots was performed using a Kodak Image Station 440CF. To determine the relative amount of opsin present in each ROS membrane specimen, the densitometric intensity of all of the immunostained components in each lane was determined and the total value was normalized to total protein load (in micrograms).

Lipid phosphorus and protein quantification

Aliquots of resuspended ROS membranes were assayed for total lipid phosphorus as described (21). Total protein content was determined using a micro-bicinchoninic acid kit, per the directions of the manufacturer (Pierce; Rockford, IL).

RNA isolation and quantitative RT-PCR analysis

Total RNA was isolated using TRI reagent (Molecular Research Center, Inc.; Cincinnati, OH). RNA yield was determined by absorbance at 260 nm, and integrity was confirmed by gel electrophoresis. Total RNA (5 μg) was converted into cDNA using the SuperScript® first-strand synthesis system for RT-PCR (Invitrogen). The cDNA samples were amplified in a Smart Cycler (Cepheid, Inc.; Sunnyvale, CA) with LightCycler® Fast-Start DNA Master SYBR Green I reagent (Roche Molecular Biochemicals; Mannheim, Germany), using specific primers (Sigma/Aldrich). Gene expression was normalized using rat GAPDH primers (F, forward primer; R, reverse primer): (F) gtcatcatctccgcccctt, (R) tttctcgtggttcacaccca. Specific primers for opsin and peripherin/rds (per-2) were designed as follows: opsin, (F) gttcgtggtccacttcacca, (R) ttggagccctggtgggtaaa; per-2, (F) gggctgttcctgaagattga, (R) ggagcatgtcgatggtcttt. The results from RT-PCR were obtained as crossing points, indicating the number of cycles required for fluorescence of the PCR product to increase above threshold value. These crossing points were converted to arbitrary units of mRNA assuming a concentration-dependent straight line for a semilog plot, with a value of 3.5 for the fold change in mRNA/cycle (slope), and the crossing point cycle number with no template as an estimate of the *y*-intercept. A final melt curve from 60°C to 95°C was performed to confirm the specificity of the PCR, and the identities of PCR products were checked by gel electrophoresis. Results were compared using a two-way ANOVA and Tukey test, with $P < 0.050$ indicating statistically significant differences.

Membrane fluidity measurements

cPA studies. Membrane fluidity was determined from steady-state anisotropy measurements as described previously (22, 23). *c*PA was introduced into ROS membrane by incubation of a membrane suspension (5.0 ml) with *c*PA in ethanol such that the final concentration of the fluorescent probe was 0.5 mol% relative to membrane phospholipid. Samples were incubated with probe or ethanol alone for 15 min at 37°C. Fluorescence anisotropy assays the rotational diffusion of a molecule from the decorrelation of polarization in fluorescence, i.e., between the exciting and emitted (fluorescent) photons. Steady-state fluorescence of *c*PA-containing ROS was recorded on a Perkin-Elmer LS55B spectrofluorimeter, equipped with polarizers, as a function of increasing temperature (28–37°C). Fluorescence intensity was recorded at $\lambda_{ex} = 324$ nm, $\lambda_{em} = 415$ nm with the excitation and emission slit-widths set at 10 and 5 nm, respectively. Unlabeled ROS preparations were used as a scattering blank. Fluorescence signal due to this scattering was subtracted from *c*PA-containing samples.

Fluorescence anisotropy was calculated using the following equation:

$$\text{Anisotropy}(r) = (I_v - I_h)/(I_v + 2I_h),$$

where I_v is the intensity parallel to the excitation plane and I_h is the emission perpendicular to the excitation plane.

DPH studies. Membranes were suspended in HEPES-buffered saline at a phospholipid concentration of 0.15 mM. A DPH stock solution was prepared in tetrahydrofuran, and 0.5 μl was added to membrane suspensions at a phospholipid:DPH mole ratio of 300:1. Fluorescence lifetime and differential polarization measurements were performed with a K2 multifrequency cross-

correlation phase fluorometer (ISS; Urbana, IL). Excitation at 351 nm was provided by an Innova 307 argon ion laser (Coherent; Santa Clara, CA). Lifetime and differential polarization data were acquired at 37°C at 15 modulation frequencies, logarithmically spaced from 5 to 150 MHz. All lifetime measurements were made with the emission polarizer at the magic angle of 54.7° relative to the vertically polarized excitation beam and with 1,4-*bis*(5-phenyloxazol-2-yl)benzene in absolute ethanol in the reference cuvette. For each differential polarization measurement, the instrumental polarization factors were measured, found to be between 1.00 and 1.05, and the appropriate correction factor applied. All measurements were repeated with each sample a minimum of three times. Total fluorescence intensity decays were analyzed with the sum of three exponential decays. Reported values are the intensity-weighted average, $<\tau>$, of the resulting three exponential time constants. Measured polarization-dependent differential phases and modulation ratios for each sample were combined with the measured total intensity decay to yield the anisotropy decay, r(t). All anisotropy decay data were analyzed using the Brownian rotational diffusion (BRD) model (14, 24) and the results were interpreted in terms of an angular distribution function of DPH, $f(\theta)$, which is symmetric about $\theta = \pi/2$. Relative phospholipid acyl chain packing was quantified using the disorder parameter, f_v, which is proportional to the overlap of the DPH orientational probability distribution, $f(\theta)\sin\theta$, with randomly oriented DPH (24, 25). The BRD model quantifies probe motion in terms of the diffusion coefficient for DPH rotation about its long axis, D_{perp}. Fluorescence anisotropy decays were also analyzed using an empirical sum-of-three-exponentials model. In this analysis, probe orientation is summarized by the order parameter S, where $S = (r_\infty/r_o)^{1/2}$ (26), and uncorrelated rotational motion is characterized by the three rotational time constants, φ_i. The three rotational time constants and their associated preexponential factors were used to calculate the weighted average rotational correlation time, $<\varphi>$. All analyses of time-resolved differential polarization data were performed with NONLIN, with subroutines specifying the fitting function written by one of the authors (D.C.M.).

Lipid extraction and fatty acid analysis

ROS membranes were protected from exposure to light as much as possible throughout processing. After thawing, a mixture containing known amounts of pentadecanoic acid (15:0), heptadecanoic acid (17:0), and heneicosanoic acid (21:0) was added to each sample as internal standards, and total lipids were extracted essentially per the Bligh–Dyer method (27), with minor modifications, as described previously (28). Lipid extracts were dried under a stream of nitrogen, and fatty acids were derivatized to form the corresponding methyl esters (FAMEs), prior to analysis by gas–liquid chromatography, essentially as described previously (28), with the following modifications. In brief, 0.20 ml of toluene and 1 ml of 2% (by vol) methanolic sulfuric acid were added to each lipid extract; the mixture was sealed in a glass tube under nitrogen atmosphere with teflon-lined caps, vortexed, and heated for 1 h at 100°C. After cooling on ice, 1.2 ml of water was added, and the FAMEs were extracted three times with 2.4 ml of hexane, then dried under nitrogen and dissolved in 20 μl nonane. Fatty acid composition was then determined by injecting 3 μl of each sample onto a DB-225 capillary column (30 m × 0.32 mm I.D.; J and W Scientific, Folsom, CA), using an Agilent 6890N gas chromatograph with a model 7683 autosampler (Agilent Technologies; Wilmington, DE), at an inlet temperature of 250°C and a split ratio of 25:1. The column temperature was programmed to begin at 160°C, ramped to 220°C at 1.33°C/min, and held at 220°C for 18 min. Hydrogen carrier gas flowed at 1.6 ml/min, and the flame ionization detector temperature was set to 270°C. The chromatographic peaks were integrated and processed with ChemStation® software (Agilent Technologies). FAMEs were identified by comparison of their relative retention times with authentic standards, and relative mole percents were calculated. Multivariant ANOVA with post-hoc Scheffe tests were used to determine statistical significance, with a maximum cutoff of $P < 0.05$.

Sterol analysis

Verification of sterol composition was achieved by reverse-phase HPLC, after saponification and extraction of the nonsaponifiable lipids, as described elsewhere (7, 8). In brief, aliquots of resuspended ROS membranes were saponified in methanolic KOH, and the nonsaponifiable lipids were extracted with petroleum ether, redissolved in methanol, and analyzed by reverse-phase HPLC (mobile phase: methanol; detection at 205 nm). An internal standard of [^{3}H]cholesterol ($\sim 1 \times 10^5$ dpm) was added to each specimen prior to saponification and extraction. Quantitative analysis of sterols was performed in comparison with authentic standards of pure 7DHC and Chol; integrated peak areas were analyzed with respect to empirically determined response factors for each sterol, with calculated masses corrected for recovery efficiency of the internal [^{3}H]cholesterol standard. This system permits baseline separation of 7DHC and Chol, with a lower detection limit of ~10 pmol.

RESULTS

AY9944 treatment causes significant alteration in sterol synthesis

Initially, we confirmed that AY9944 had produced the desired and expected effect on sterol metabolism in the rat under the given treatment conditions, which would be reflected in the abnormal steady-state accumulation of 7DHC and reduction of both Chol levels as well as total sterol levels in serum (**Table 1**). This expectation was met: after 1 month of AY9944 treatment, the 7DHC:Chol molar ratio in serum was 2.0 and total sterols were only 16.4% of control values; by 3 months of AY9944 treatment, the 7DHC:Chol molar ratio was 4.6, and the total sterols were

TABLE 1. Sterol composition and content of serum and ROS membranes from AY9944-treated and control rats

	Treatment Group	Age	7DHC:Chol	Total Sterols	Control
		month (N)	*mole ratio*	*mg/dl*	*%*
Serum	Control	1 (7)	0	100.5 ± 10.7	100
	+AY9944	1 (19)	2.0 ± 0.8	16.5 ± 6.2	16.4
	Control	3 (12)	0	95.5 ± 17.5	100
	+AY9944	3 (16)	4.6 ± 1.0	20.8 ± 5.6	21.8
ROS	Control	1 (4)	0		
	+AY9944	1 (6)	3.5 ± 0.4		
	Control	3 (6)	0		
	+AY9944	3 (4)	5.6 ± 1.6		

7DHC, 7-dehydrocholesterol; Chol, cholesterol; ROS, rod outer segment. Aliquots (50 μl each) of serum or ROS membranes (resuspended in buffer) were saponified in methanolic KOH, and the nonsaponifiable lipids were extracted with petroleum ether, evaporated to dryness, redissolved in methanol, and analyzed by reverse-phase HPLC. Values represent the mean ± SD, with number of biologically independent samples (N) given in parentheses, corrected for recovery efficiency using an internal standard of [^{3}H]cholesterol.

21.8% of control values. In control rats, 7DHC levels were below the limit of detection using the HPLC method employed (<10 pmol), so the 7DHC:Chol ratio is 0 in control serum. A similar analysis of ROS membrane sterols revealed that the 7DHC:Chol molar ratio was 3.5 after 1 month of AY9944 treatment, and after 3 months, the ratio had increased 1.6-fold ($P < 0.05$) to 5.6. There was no detectable 7DHC in control ROS preparations. These findings are in good agreement with the results of our prior studies (7, 8) and confirm that the effects of AY9944 were as expected and increased with duration of exposure.

AY9944 treatment causes profound perturbation of ROS membrane fatty acid composition

The results of the comparative fatty acid analysis of ROS membranes at 1 and 3 postnatal months as a function of AY9944 treatment are shown in **Fig. 1**. Here, the values are expressed as relative mole percent of the total recovered fatty acid. In good agreement with reports by others (as reviewed in Ref. 29), the major ROS membrane fatty acid species are 22:6n3 >> 18:0 > 16:0 >> 18:1 ~20:4n6. As shown in Fig. 1A, after 1 month of AY9944 treatment, there was no statistically significant reduction in the level of 22:6n3 (DHA), compared with that found in ROS membranes from age-matched control rats. However, there was a 3.6-fold increase in the levels of 22:5n6 in ROS membranes from AY9944-treated rats, relative to controls (5.8 mol% vs. 1.6 mol%, respectively; $P < 0.05$), but the mass of 22:5n6 is relatively minor, especially when compared with that of 22:6n3. Several other fatty acid species exhibited alterations as a function of AY9944 treatment compared with controls; however, the magnitude of these changes, as well as their mass (relative mole percent), was relatively small. The ratio of n6 to n3 fatty acids was 0.60 ± 0.02 for ROS membranes from AY9944-treated rats, versus 0.39 ± 0.10 for controls, but this difference was not statistically significant ($P > 0.05$). After 3 months of AY9944 treatment (Fig. 1B), there was a significantly lower level of 22:6n3 in ROS membranes compared with age-matched controls (24.9 mol% vs. 39.4 mol%; 1.58-fold difference, $P < 0.05$); this was accompanied by a 4.5-fold higher level of 22:5n6 (5.4 mol%) compared with age-matched controls (1.2 mol%; $P < 0.001$). The n6:n3 ratio was 0.52 ± 0.05 for ROS membranes from AY9944-treated animals, versus 0.22 ± 0.09; this 2.36-fold difference was highly significant ($P < 0.001$). Perhaps more informative is the saturation index, R_s, which we define as the ratio of saturated fatty acid species to PUFAs (defined here as any fatty acid containing two or more double bonds). After 1 month of AY9944 treatment R_s was 0.89 versus 0.91 for age-matched controls (i.e., only a ~2% difference), whereas after 3 months of treatment, R_s was 1.27 versus 1.13 for age-matched controls (a ~12% difference). More importantly, if we compare the R_s value at 1 versus 3 months of AY9944 treatment, there was a ~1.4-fold increase in the saturation index of ROS membrane lipids, which would predict a significant decrease in membrane fluidity as a function of increasing time of exposure to AY9944.

If one normalizes the levels of three prominent resident ROS membrane PUFAs (20:4n6, 22:5n6, and 22:6n3) to the levels of stearic acid (18:0), which do not vary as a function of AY9944 treatment, the following information is revealed (**Table 2**). At 1 month of AY9944 treatment, the normalized levels of arachidonic acid (20:4n6) modestly increased (by about 16%), relative to controls, and this change was statistically significant (per data in Fig. 1; $P < 0.05$), whereas by 3 months, the apparent change in the relative level of this fatty acid was not statistically significant. The normalized levels of 22:6n3 (DHA) after 1 month of AY9944 treatment were not statistically different from those of age-matched control membranes, but then dramatically decreased (by ~41%, $P < 0.05$), relative

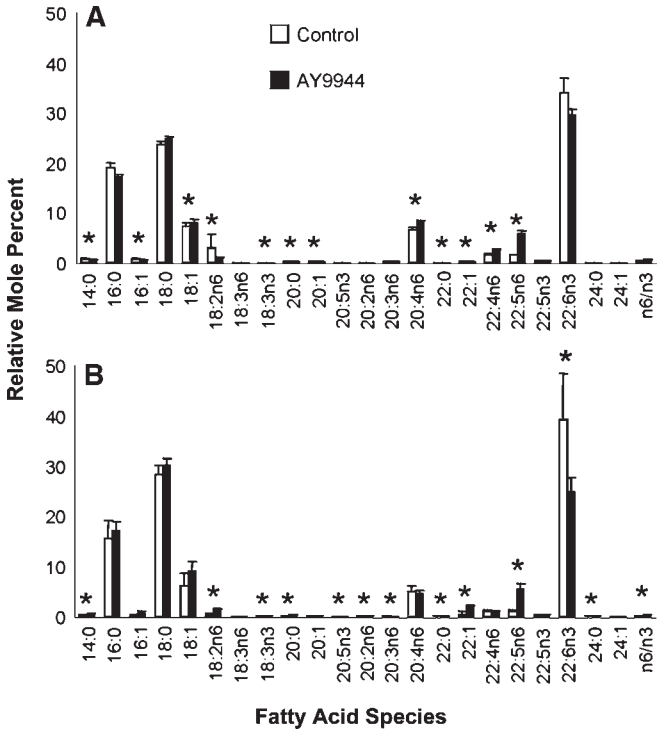

Fig. 1. Fatty acid profiles of retinal rod outer segment (ROS) membranes from AY9944-treated (filled bars) and control (open bars) rats at (A) 1 and (B) 3 postnatal months of age. Values are mean ± SD (N = 3), expressed as relative mole percent. * Statistical significance ($P < 0.05$; multivariant ANOVA with post-hoc Scheffe test) of differences between treated and control values for a given fatty acid species.

TABLE 2. Normalized PUFA content of ROS membranes from control and AY9944-treated rats

	1 Month Normalized Value			3 Months Normalized Value		
Fatty Acid	Control	+AY9944	Change	Control	+AY9944	Change
			%			%
20:4n6	0.286	0.333	+16.4[a]	0.181	0.155	−14.4[b]
22:5n6	0.067	0.233	+348[a]	0.041	0.180	+439[a]
22:6n3	1.44	1.19	−17.9[b]	1.39	0.825	−40.6[a]

Data are average values, obtained by dividing the relative mol% values (see Fig. 1) of the given fatty acid species by the relative mol% of stearic acid (18:0).

[a] Statistically significant ($P < 0.05$; N = 3).

[b] Not statistically significant ($P > 0.05$; N = 3).

to age-matched controls, after 3 months of AY9944 treatment. The normalized levels of eicosapentaenoic acid (22:5n6) exhibited a marked (almost 3.5-fold) increase after 1 month of AY9944 treatment, relative to controls, with an even larger (4.4-fold) elevation occurring after 3 months of treatment ($P < 0.05$). Again, it should be appreciated that whereas DHA represents the major fatty acid in ROS membranes, 20:4n6 and 22:5n6 represent quantitatively minor species, normally accounting for only about 5–6 mol% and 2–3 mol%, respectively, of the total fatty acid content of ROS membranes (29). Thus, although the apparent changes in the levels of these minor fatty acids may be statistically significant, it is unlikely that such changes would significantly impact the physical properties of the membranes. However, the large decrease in DHA content at 3 months would be expected to have significant consequences on membrane properties (see Discussion). These changes are also consistent with our recent observations concerning reduced levels of DHA in whole retinas of rats treated with AY9944, relative to age-matched controls (9).

AY9944 treatment does not alter the lipid:protein ratio or opsin content of ROS membranes

The visual pigment apoprotein opsin accounts for at least 90% of the total integral membrane protein content of ROS membranes (as reviewed in Ref. 29). To assess whether AY9944 treatment had any effect on protein packing density in ROS membranes, we measured lipid phosphorus and total protein in ROS membranes from treated and control rats, and also performed quantitative immunoblot analysis of those membranes, using monospecific antibodies (mAb 4D2) against opsin. The average phospholipid:protein ratios were not appreciably different in ROS membranes prepared from AY9944-treated rats [N = 2: 1 month, 58 (range, 53.1–62.9); and 3 months, 56 (range, 52.3–59.7)] compared with controls [1 month, 55 (range, 54.7–60.3); and 3 months, 57 (range, 52.2–61.8)]. Also, Western analysis (**Fig. 2A, B**) of ROS membranes prepared from 1 and 3 month-old, AY9944-treated and age-matched control rats showed no apparent differences in the levels of opsin as a consequence of AY9944 treatment. Consistent with this, we also found no effect of AY9944 treatment on opsin mRNA expression levels (by quantitative RT-PCR) (Fig. 2C), or on mRNA expression levels of peripherin/rds, another ROS resident membrane protein (data not shown). Taken together, these data suggest that AY9944 treatment does not appreciably alter the protein packing density in ROS membranes or alter opsin expression or incorporation into ROS membranes.

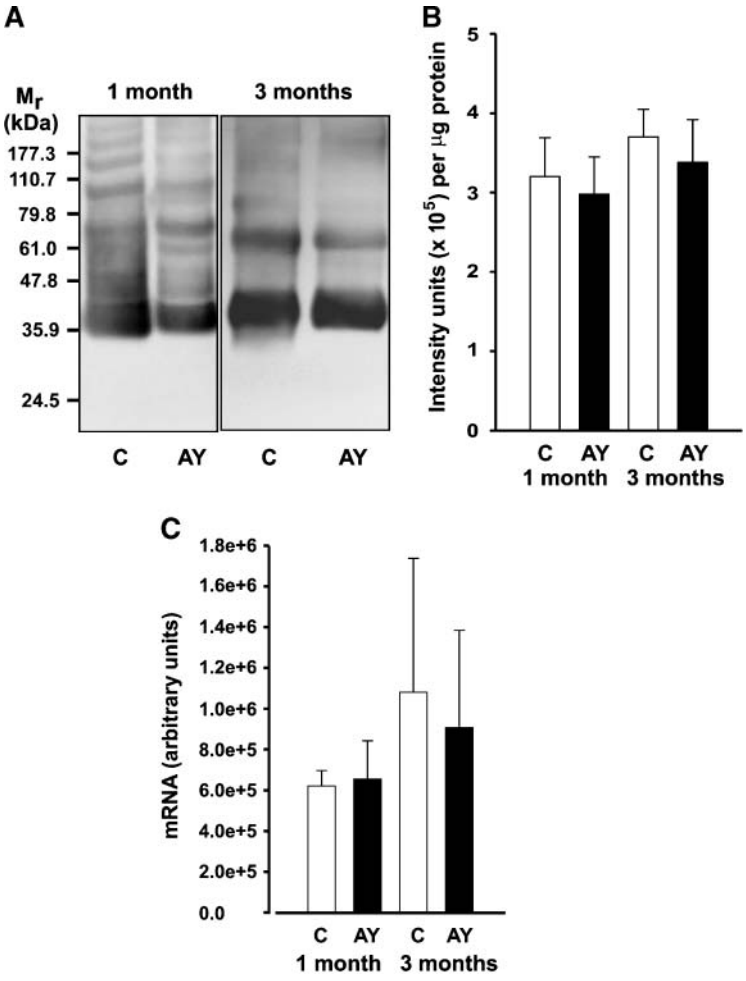

Fig. 2. Opsin protein levels in control (C) and AY9944-treated (AY) rat ROS membranes. A: Western blot probed with monoclonal anti-opsin antibodies (mAb 4D2). Samples were adjusted in order to load an equivalent amount (1 mg total) of lipid phosphorus per lane. Immunoreactivity was visualized using HRP-conjugated secondary antibodies and enhanced chemifluorescence detection. Migration positions of protein molecular weight markers (M_r in kDa) are indicated at left. B: Quantitative densitometric analysis of Western blots. Graph represents measurements (mean ± SD) obtained from four independent blots per treatment and time point (1 and 3 months). C: Quantitative RT-PCR analysis of opsin expression in retinas isolated from control and AY9944-treated rats. Graph shows values (mean ± SD, N = 4) expressed in arbitrary units.

AY9944 treatment causes alterations in the physical properties of ROS membranes

Given the fact that there were dramatic alterations in the sterol and fatty acid profiles of ROS membranes as a consequence of AY9944 treatment, we evaluated whether the physical properties of the membranes also were altered by such treatment. A comprehensive examination of the effects of treatment with AY9944 on acyl chain packing (fluidity) in ROS membranes was performed utilizing steady-state fluorescence anisotropy of *c*PA and fluorescence lifetime and anisotropy decay measurements of DPH. These two fluorescent probes partition into different parts of a fluid phase membrane, with *c*PA anchored to the interface whereas DPH is free to partition into the center of the bilayer, where its orientation will reflect the free volume resulting from the degree of acyl chain packing order (10).

When used at a suitably low concentration, *c*PA is sensitive to changes in membrane order in the interfacial region. We compared the fluorescence anisotropy of *c*PA in ROS membranes from control and AY9944-treated rats in vitro as a function of age (1 vs. 3 months) at 37°C. The results are shown in **Fig. 3**. ANOVA analysis of the anisotropy data revealed no statistically significant alteration in fluorescence anisotropy in ROS membranes from 1 month-old AY9944-treated rats, relative to age-matched controls. However, at 3 months of age, there was a modest (~14%) decline in the anisotropy in ROS from AY9944-treated rats, relative to controls, which was statistically significant ($P = 0.0068$, N = 4), consistent with an increase in fluidity in the interfacial region.

We performed a follow-up analysis of ROS membranes from 3 month-old AY9944-treated and control animals, using DPH as the fluorescent membrane probe. DPH fluorescence is efficiently quenched by water; hence, DPH fluorescence lifetime in a membrane is indicative of relative water penetration (13). In control ROS membranes at 37°C, the intensity-weighted average fluorescence lifetime, $<\tau>$, was 9.36 ± 0.05 ns, whereas in ROS membranes from AY9944-treated animals, it was significantly lower (9.17 ± 0.1 ns; $P = 0.017$). This numerically modest (~2%) yet statistically significant decrease in fluorescence lifetime is consistent with the interpretation that the headgroup region in the treated membranes is more loosely packed with respect to permitting transient water penetration. Taken together with the change in *c*PA fluorescence anisotropy, these results indicate that the interfacial and headgroup regions of the membrane are more disordered in the ROS membranes from AY9944-treated rats, compared with ROS membranes from age-matched control rats.

The decay of DPH fluorescence anisotropy reflects the influence of acyl chain packing on DPH motion and orientational order in the hydrophobic core of the membrane (13, 14). As shown in **Fig. 4**, in this region, the ROS membranes from AY9944-treated rats exhibited increased acyl order relative to age-matched (3 month-old) controls. The BRD model explicitly separates the distinct effects of probe orientational order and probe motion on the dynamics of fluorescence depolarization. The DPH orientational distribution is summarized by the disorder parameter

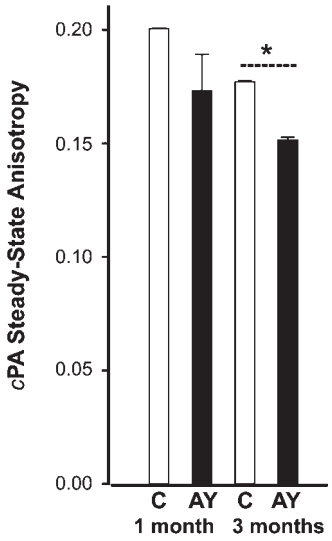

Fig. 3. Steady-state anisotropy measurements of *cis*-parinaric acid (*c*PA) in purified ROS membranes from 1 and 3 month-old rats. Open bars, controls; filled bars, AY9944-treated. Values are mean ± SD (N = 4), measured at 37°C. * Statistically significant difference ($P = 0.0068$) between treated versus control samples at 3 months of age.

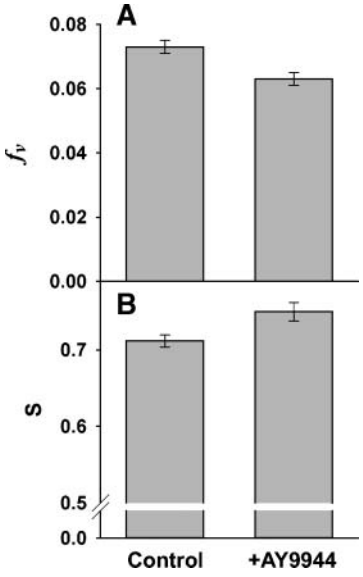

Fig. 4. Measures of acyl chain ensemble order (membrane fluidity) obtained from analysis of 1,6-diphenyl-1,3,5-hexatriene (DPH) fluorescence anisotropy decays. A: The free volume (or disorder parameter), f_v, from analysis via the Brownian rotational diffusion (BRD) model. The smaller value for the membranes from AY9944-treated animals, compared with controls, indicates decreased acyl chain packing disorder ($P < 0.001$, N = 6). B: The order parameter, S, calculated from the model-independent analysis of the anisotropy decays in terms of the sum of three exponential decays. The higher S value for the membranes from AY9944-treated animals, compared with controls, indicates increased orientational order of DPH ($P < 0.001$, N = 6). Error bars indicate ± SD.

f_v, and this parameter was significantly reduced in the treated ROS membranes, relative to controls (Fig. 4A). Increased order in the treated ROS membranes is also reported by the model-independent analysis, which summarizes orientational order as indicated by the order parameter, S (Fig. 4B). The relative changes in both parameters may appear to be modest (range, 6–13%), but both parameters indicate a substantial increase in acyl chain order (reduced fluidity) in the core of the membrane. For a biological membrane at 37°C, a similar reduction in fluidity would require an increase in Chol from 12 mol% to ~30 mol%, or a reduction in temperature from 37°C to ~25°C. A comparable reduction of f_v was observed in ROS membranes from rats raised on an n3-deficient diet, which caused a substantial reduction in the levels of 22:6n3 (30).

A second indication that the core of the bilayer is less fluid in the ROS membranes from AY9944-treated rats is the reduced rate of DPH rotational motion in these membranes. Changes in both the diffusion constant for DPH rotation about its long axis, D_{perp}, from the BRD analysis (**Fig. 5A**), and the average rotational time constant, $<\varphi>$, from the empirical analysis (Fig. 5B) demonstrate that probe motion is slower in the treated ROS membranes. Both parameters of rotational motion change about 15%, but significant perturbations, such as a 2.5-fold increase in Chol or a 10–15°C reduction in temperature, would be required to produce a comparable reduction in probe motion.

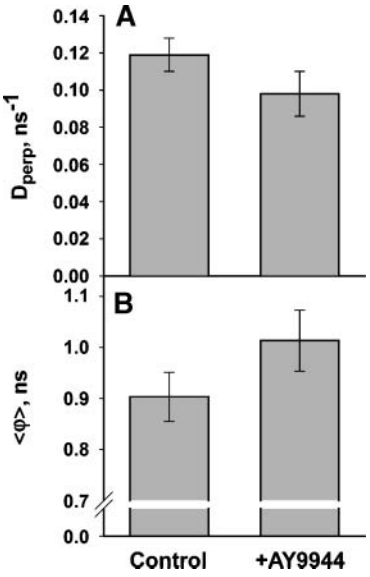

Fig. 5. Measures of DPH rotational motion obtained from analysis of DPH fluorescence anisotropy decays. A: The diffusion constant for DPH rotation about its long axis, D_{perp}, from the BRD model analysis. The smaller value in ROS membranes from the AY9944-treated animals, compared with controls, indicates slower DPH rotation (P = 0.006, N = 6). B: The weighted average of the three empirical rotational time constants, $<\varphi>$, from the model–independent analysis. The higher value for membranes from AY9944-treated animals, compared with controls, indicates slower DPH rotation (P = 0.006, N = 6). Error bars indicate ± SD.

AY9944 treatment alters regenerability of rhodopsin

The changes in the membrane environment that occur at 3 months are concomitant with the previously described retinal degeneration in this model (8), which also entails defective phototransduction. To determine whether AY9944-induced alterations in membrane dynamics are correlated with a parameter pertinent to phototransduction (e.g., rhodopsin function), we next analyzed the ability of the bleached photopigment (opsin) to recombine with exogenously supplied 11-*cis* retinal chromophore to regenerate rhodopsin in vitro, using ROS membranes from control versus AY9944-treated rats. As shown in **Fig. 6**, at 1 postnatal month, no significant decrease in rhodopsin regenerability was observed between ROS obtained from control and AY9944-treated rat retinas (95 ± 2.6% in controls, 92 ± 1.5% in AY9944-treated retinas). The total extent and rate of rhodopsin regeneration, however, were decreased significantly by 3 postnatal months as a function of AY9944 treatment (65 ± 1.5% regenerability) relative to controls (82 ± 3.0% regenerability).

DISCUSSION

In the present study, we have demonstrated that perturbation of sterol biosynthesis by use of the distal pathway inhibitor AY9944 profoundly alters both ROS membrane sterol composition as well as fatty acid composition, relative to age-matched control rats, in a time-dependent manner. Concomitantly, as expected, the physical properties of the membranes are altered; notably, there is a significant reduction in membrane fluidity by 3 months, as measured by use of fluorescent fatty acid probes. Also, the ability of opsin to combine with its 11-*cis* retinal chromophore to

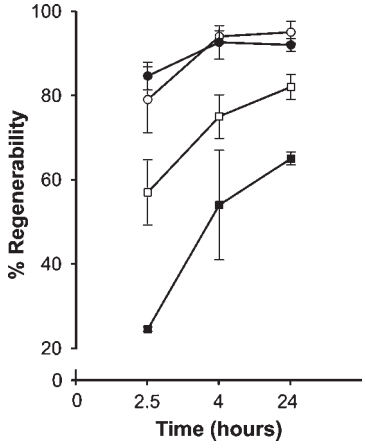

Fig. 6. Rhodopsin regeneration in ROS membranes from control and AY9944-treated rats. Values expressed as percent regeneration, shown as a function of time ROS membranes were incubated with excess 11-*cis* retinal at 37°C. Comparison of values from 1 month-old control (open circles) versus AY9944-treated rats (filled circles) shows no statistically significant difference (N = 3). In contrast, comparison of values from 3 month-old control (open squares) and AY9944-treated rats (filled squares) showed a statistically significant difference (P = 0.0006, N = 3, at 24 h). Error bars indicate ± SD.

regenerate rhodopsin is compromised by 3 months of treatment. Interestingly, although the changes in membrane sterol and fatty acid composition are substantial even by 1 month of treatment, there is no retinal degeneration or profound electrophysiological deficits at this stage in the treatment time course (7), nor is rhodopsin regeneration affected. By 3 months of AY9944 treatment, however, ROS sterol and fatty acid composition are even more deranged, most notably with the profound (>40%) loss in DHA content, and rhodopsin regenerability is significantly compromised. This stage of treatment corresponds to the progression to marked retinal degeneration, particularly rod photoreceptor degeneration and death, as well as defective rod and cone visual function (8). The question arises as to whether the observed effects on membrane fluidity and visual pigment regenerability are due primarily to the altered sterol composition or to the altered fatty acid composition of the ROS membranes. To answer this question, one must consider in further detail the changes in these two distinct lipid classes.

Because the absolute recovery efficiency of ROS membranes varies from one preparation to the next, one cannot confidently make direct comparisons of absolute values for sterol mass between membrane preparations. However, if one normalizes the total sterol mass to total fatty acid mass on a molar basis, a comparison can be made. Using the empirically determined values for the total sterol and fatty acid content of ROS membranes from both AY9944-treated and control rats, we calculate a sterol: fatty acid mole ratio of 0.062 (±12%). This is in good agreement with published values for both the Chol content (~8–10 mol% of total ROS lipid) and phospholipid content (~85–90 mol% of total ROS lipid, and 65–75 mol of phospholipid per mole of rhodopsin) of ROS membranes, (as reviewed in Ref. 29). To a first approximation (excluding plasmalogens), each glycerophospholipid molecule contains two acyl chains. Hence, if the Chol: phospholipid mole ratio is approximately 1:9 in ROS membranes, the Chol:fatty acid mole ratio should be about 1:18, or 0.056. The fact that this ratio is the same in ROS membranes from both normal control and AY9944-treated rats further reveals that the total sterol mass in ROS membranes is unaffected by AY9944 treatment (i.e., there is no net loss of sterol mass in the membranes). Hence, there is a one-for-one molecular replacement of Chol with 7DHC under the conditions employed. However, the chemical composition of the membrane sterol pool is dramatically and progressively altered: by 1 month of AY9944 treatment, the 7DHC:Chol mole ratio is 3:5, whereas by 3 months, it is 5:6; in contrast, Chol is essentially the only sterol present in normal rat ROS membranes at any age.

The impact of sterol chemistry on the structure and function of biological membranes has been a subject of extensive investigation over the years (as reviewed in Refs. 31, 32). In sum, there do not appear to be uniformly applicable rules to predict with certainty the consequences of replacing Chol with sterols of different structures, such as 7DHC; rather, the impact of such changes tends to be a function of the particular sterol and the biological system being examined. However, recent studies from our lab using model membrane systems suggest that 7DHC has physical properties very similar to those of Chol, including packing densities and molecular volumes in mixed sterol-phospholipid monolayers (Langmuir films) (33, 34). These findings, in conjunction with the fact that sterols account for <10 mol% of the total lipid in ROS membranes (29), would tend to support the conclusion that altered sterol composition is not a major factor in the observed changes in membrane fluidity or rhodopsin regenerability.

Our results obtained with fluorescent probe measurements demonstrate that the hydrophobic core of the ROS membranes becomes more ordered (less fluid), as has been previously reported in cases in which there is a substantial decrease in the polyunsaturated fatty acid (e.g., 22:6n3) content of the ROS membrane (30). In a study of the effects of dietary n3 deficiency, a similar increase in the acyl chain order reported by DPH in ROS membranes was accompanied by a 50% increase in the time required for transducin binding to light-activated rhodopsin and a 3-fold decrease in light-stimulated phosphodiesterase activity (30). An earlier study of the relationship between acyl chain packing, as reported by f_v, and formation of the light-activated conformation metarhodopsin II indicates that the decrease in f_v found in the present study would depress metarhodopsin II by 25–30% (35). Increasing Chol in ROS disk membranes from 12% to 30% produced a reduction of f_v comparable to treatment with AY9944, and this was accompanied by a 20% reduction in metarhodopsin II (36). In all of these earlier studies, increased acyl chain order in the membrane hydrophobic core was accompanied by an increase in DPH fluorescence lifetime, indicating increased order in the head group region. In the present study, the decreased order in the headgroup/interfacial region reported by both DPH and *c*PA strongly suggests that treatment with AY9944 produces a unique set of changes in the physical properties of ROS membranes. In the core of the membrane, these changes appear to be dominated by the marked reduction in the number of 22:6n3 acyl chains, consistent with the increased order and decreased motion of DPH (Figs. 4, 5, respectively). However, the changes reported by *c*PA (Fig. 3) and DPH fluorescence lifetime suggest additional significant modifications of membrane architecture. This simultaneous decrease in fluidity in the membrane core and slight increase in fluidity in the headgroup/interfacial region may be due to the particular molecular species that lost 22:6n3 acyl chains, or a change in lipid lateral phase organization.

Our fatty acid analyses (Fig. 1) showed that although there were several ROS fatty acyl species that exhibited statistically significant altered levels, comparing AY9944-treated rats to age-matched controls, the magnitude of these changes tended to be rather modest for most species, particularly for saturated and monounsaturated acyl chains. The spectroscopic results obtained with *c*PA indicate that these changes were not substantial enough to appreciably alter membrane fluidity after only 1 month of AY9944 treatment. However, more-dramatic alterations

in ROS membrane fatty acid composition were observed by 3 months of AY9944 treatment, relative to age-matched controls. Notably, by normalizing the 22:6n3 content to that of 18:0, an invariant fatty acid (Table 2), there was a ~41 mol% loss of 22:6n3, compared with controls. This finding is consistent with the results obtained recently by lipidomic analysis of whole retinas from AY9944-treated and control rats, where the most notable alteration in retinal glycerophospholipids (phosphatidylethanolamine, phosphatidylcholine, and phosphatidylserine) was a profound loss in molecular species containing 22:6n3 with AY9944 treatment (9). Clearly, the magnitude of this change was sufficient to cause appreciable changes in the physical properties of the ROS membranes (Figs. 3–5).

Increased order in the membrane core and simultaneous decreased order in the headgroup and interfacial regions is somewhat unique and suggests that other changes in membrane composition also play a role in altering the membrane. Significantly large alterations in the protein-to-lipid ratio would result in marked differences in the physical properties of the membranes, which would be readily detectable by the spectroscopic methods employed here. In the case of the ROS membrane, the visual pigment rhodopsin is estimated to account for at least 90% of the total integral membrane protein, and the lipid-to-protein mass ratio is approximately 1:1 (29). Rhodopsin packing density also has been correlated with alterations in membrane function (assessed by rhodopsin activation, which impacts efficiency of the phototransduction cascade) (37, 38). However, our analyses showed that there was no significant alteration in the opsin-to-phospholipid ratio of ROS from AY9944-treated rats, compared with age-matched controls; hence, the protein packing density in ROS membranes was unaffected by AY9944 treatment. In fact, a reduction in opsin levels, and concomitant reduction in protein packing density, would be predicted to cause an increase in membrane fluidity, which clearly was not observed here.

It is important to note that although no histological degeneration or apparent loss in rod or cone electrophysiological responsiveness was observed in the AY9944-induced rat model of SLOS after 1 month of treatment, there was an appreciable and statistically significant delay in the timing of those photoresponses (i.e., increased implicit times) (7). The implicit time is related to the efficiency of the phototransduction cascade operative in the photoreceptor cell, involving both the protein components organized within and at the surface of the ROS disk membranes as well as the cyclic nucleotide-gated ion channels located in the ROS plasma membrane (39). Hence, it is apparent that even the relatively modest (in absolute magnitude) changes in the fatty acid profile of the ROS membranes that occur by 1 month of AY9944 treatment have some biological impact at the membrane level, although not enough to cause overt cellular dysfunction or degeneration. The retina requires high levels of DHA for optimal function, particularly with regard to supporting photoreceptor viability and electrophysiological competence (29). ROS membranes in which the DHA content has been significantly reduced compared with normal levels exhibit slower than normal photoresponses, which correlates with impaired activation of transducin, the cognate G-protein and key player in the phototransduction cascade (30). It is tempting to speculate that faced with a metabolic insult (such as disrupting normal Chol biosynthesis), the cell responds by globally remodeling its membrane lipidome in an effort to preserve cellular integrity and function, including preservation of membrane fluidity that is critical to the function of a host of membrane-associated enzymes, receptors, and ion channels (40). However, although the retinal photoreceptor cells may be able to tolerate this level of stress for at least 1 month, eventually they lose physiological competence and cellular integrity, undergoing degeneration and cell death by 3 months of exposure to AY9944 (8, 15). At that point, rod and cone electrophysiology and structure are severely compromised, and this also correlates temporally with the dramatic losses in the DHA content of ROS membranes documented in this study, as well as those recently reported under virtually identical conditions for whole retina (9). Notably, it is at 3 months of AY9944 treatment that we also observe altered membrane properties, as assessed by the behavior of fluorescent probes added in small amounts to isolated ROS membranes, which also are consistent with the more dramatic changes in fatty acid composition, particularly DHA.

Herein, we show for the first time that one pathologic consequence of decreased Chol biosynthesis in a rat model of SLOS is reduced rhodopsin regenerability. It should be noted that our in vitro studies of rhodopsin regeneration were performed in the presence of excess exogenous 11-*cis* retinal; hence, the decreased regeneration cannot be due to insufficient retinoid availability. Reduction in the regenerability of rhodoposin also would be expected to negatively impact the efficiency of phototransduction and, hence, photoreceptor function, consistent with our prior in vivo observations with the SLOS rat model (7, 8, 15). We speculate that opsin's ability to assume a conformational state requisite for optimal regeneration is impaired as a consequence of alterations in membrane lipid composition and biophysical properties (e.g., fluidity), such alterations being more extensive by 3 months than by 1 month of exposure of rats to AY9944. This may represent a threshold phenomenon: beyond some level of deviation from normal membrane composition and biophysical properties, opsin regenerability is compromised, whereas deviations below that level (even though not normal) are apparently tolerable with respect to opsin regenerability. A similar hypothesis (the molecular spring model) was put forward by Dratz and Holte (41) to explain diminished rhodopsin bleaching kinetics in the presence of altered levels of Chol and DHA. Whether an analogous mechanism involving lipid–protein interactions in rhodopsin regeneration is at play here is unknown. However, we suggest that alterations in membrane composition that decrease headgroup/interfacial order and increase hydrocarbon order also result in decreased efficiency of rhodopsin regeneration, consistent with the observed

electrophysiological defects in the SLOS rat model and in human SLOS patients, and may contribute to long-term retinal degeneration due to the inability of the retina to adapt to the continuous exposure to light.

With the exception of our recent studies with the SLOS rat model (9), the implication of a linkage between disrupted sterol biosynthesis and altered fatty acid metabolism, particularly in association with SLOS, has never been proposed. We have proposed (9) that cross-talk between sterol and fatty acid metabolism may explain the results observed with the AY9944-induced rat model, and that additional metabolic compromise beyond the primary defect in sterol biosynthesis may contribute to the pathology of SLOS. The exact mechanism by which AY9944 (which allegedly is a selective inhibitor of DHCR7 in the sterol pathway) perturbs fatty acid metabolism remains to be elucidated. Interestingly, altered membrane fluidity has been reported recently by one of us (K.B-B.) in a study of skin fibroblasts obtained from SLOS patients, using the same spectroscopic techniques as employed in the current study (42). Although this finding had been considered only within the context of altered membrane sterol composition, our results suggest the possibility that additional changes in the steady-state fatty acid composition of the fibroblast membranes also may underlie the observed alterations in membrane fluidity.

REFERENCES

1. Kelley, R. I., and G. E. Hermann. 2001. Inborn errors of sterol biosynthesis. *Annu. Rev. Genomics Hum. Genet.* **2:** 299–341.
2. Porter, F. D. 2003. Human malformation syndromes due to inborn errors of cholesterol synthesis. *Curr. Opin. Pediatr.* **15:** 607–613.
3. Smith, D. L., L. Lemli, and J. M. Opitz. 1964. A newly recognized syndrome of multiple congenital anomalies. *J. Pediatr.* **64:** 210–217.
4. Correa-Cerro, L. S., and F. D. Porter. 2005. 3Beta-hydroxysterol delta7-reductase and the Smith-Lemli-Opitz syndrome. *Mol. Genet. Metab.* **84:** 112–126.
5. Elias, E. R., R. M. Hansen, M. Irons, N. B. Quinn, and A. B. Fulton. 2003. Rod photoreceptor responses in children with Smith-Lemli-Opitz syndrome. *Arch. Ophthalmol.* **121:** 1738–1743.
6. Kolf-Klauw, M., F. Chevy, C. Wolf, B. Siliart, D. Citadelle, and C. Roux. 1996. Inhibition of 7-dehydrocholesterol reductase by the teratogen AY9944: a rat model for Smith-Lemli-Opitz syndrome. *Teratology.* **54:** 115–125.
7. Fliesler, S. J., M. J. Richards, C-Y. Miller, and N. S. Peachey. 1999. Marked alteration of sterol metabolism and composition without compromising retinal development or function. *Invest. Ophthalmol. Vis. Sci.* **40:** 1792–1801.
8. Fliesler, S. J., N. S. Peachey, M. J. Richards, B. A. Nagel, and D. K. Vaughan. 2004. Retinal degeneration in a rodent model of Smith-Lemli-Opitz syndrome: electrophysiologic, biochemical, and morphologic features. *Arch. Ophthalmol.* **122:** 1190–1200.
9. Ford, D. A., J. K. Monda, R. S. Brush, R. E. Anderson, M. J. Richards, and S. J. Fliesler. 2008. Lipidomic analysis of the retina in a rat model of Smith-Lemli-Opitz syndrome: alterations in docosahexaenoic acid content of phospholipid molecular species. *J. Neurochem.* **105:** 1032–1047.
10. Lentz, B. R. 1993. Use of fluorescent probes to monitor molecular order and motions within liposome bilayers. *Chem. Phys. Lipids.* **64:** 99–116.
11. Drummen, G. P. C., J. A. F. Op den Kamp, and J. Post. 1999. Validation of the peroxidative indicators, *cis*-parinaric acid and parinaroylphospholipids, in a model system and cultured cardiac myocytes. *Biochim. Biophys. Acta.* **1436:** 370–382.
12. Trevors, J. T. 2003. Fluorescent probes for bacterial cytoplasmic membrane research. *J. Biochem. Biophys. Methods.* **57:** 87–103.
13. Zannoni, C., A. Argioni, and P. Cavatorta. 1983. Fluorescence depolarization in liquid crystals and membrane bilayers. *Chem. Phys. Lipids.* **32:** 179–250.
14. van der Meer, B. W., H. Pottel, W. Herreman, M. Ameloot, H. Hendricks, and H. Schroder. 1984. Effect of orientational order on the decay of the fluorescence anisotropy in membrane suspensions. *Biophys. J.* **46:** 515–523.
15. Fliesler, S. J., D. K. Vaughan, E. C. Jenewein, M. J. Richards, B. A. Nagel, and N. S. Peachey. 2007. Partial rescue of retinal function and sterol steady-state in a rat model of Smith-Lemli-Opitz syndrome. *Pediatr. Res.* **61:** 273–278.
16. Fliesler, S. J., R. Florman, and R. K. Keller. 1995. Isoprenoid lipid metabolism in the retina: dynamics of squalene and cholesterol incorporation and turnover in frog rod outer segment membranes. *Exp. Eye Res.* **60:** 57–69.
17. Fliesler, S. J., M. J. Richards, C. Y. Miller, and R. J. Cenedella. 2000. Cholesterol synthesis in the vertebrate retina: effects of U18666A on rat retinal structure, photoreceptor membrane assembly, and sterol metabolism and composition. *Lipids.* **35:** 289–296.
18. Cusanovich, M. 1982. Kinetics and mechanism of rhodopsin regeneration with 11-*cis*-retinal. *Methods Enzymol.* **81:** 443–447.
19. Boesze-Battaglia, K., H. Song, M. Sokolov, C. Lillo, L. Pankoski-Walker, C. Gretzula, B. Gallagher, R. A. Rachel, N. A. Jenkins, N. G. Copeland, et al. 2007. The tetraspanin protein peripherin-2 forms a complex with melanoregulin, a putative membrane fusion regulator. *Biochemistry.* **46:** 1256–1272.
20. Towbin, H., T. Staehelin, and J. Gordon. 1979. Electrophoretic transfer of proteins from polyacrylamide gels to nitrocellulose sheets: procedure and some applications. *Proc. Natl. Acad. Sci. USA.* **76:** 4350–4354.
21. Bartlett, G. R. 1959. Phosphorus assay in column chromatography. *J. Biol. Chem.* **234:** 466–468.
22. Sklar, L. A., B. S. Hudson, M. Petersen, and J. Diamond. 1977. Conjugated polyene fatty acids as fluorescent probes: spectroscopic characterization. *Biochemistry.* **16:** 813–819.
23. Calafut, T., J. Dix, and A. Verkman. 1989. Fluorescence depolarization of *cis*-and *trans*-parinaric acids in artificial and red cell membranes. *Biochemistry.* **21:** 5051–5058.
24. Mitchell, D. C., and B. J. Litman. 1998. Molecular order and dynamics in bilayers consisting of highly polyunsaturated phospholipids. *Biophys. J.* **74:** 879–891.
25. Straume, M., and B. J. Litman. 1987. Equilibrium and dynamic structure of large, unilamellar, unsaturated acyl chain phosphatidylcholine vesicles. Higher order analysis of 1,6-diphenyl-1,3,5-hexatriene and 1-[4-(trimethylammonio) phenyl]-6-phenyl-1,3,5-hexatriene anisotropy decay. *Biochemistry.* **26:** 5113–5120.
26. Heyn, M. P. 1979. Determination of lipid order parameters and rotational correlation times from fluorescence depolarization experiments. *FEBS Lett.* **108:** 359–364.
27. Bligh, E. J., and W. J. Dyer. 1959. A rapid method of total lipid extraction and purification. *Can. J. Biochem. Physiol.* **37:** 911–917.
28. Martin, R. E., M. H. Elliott, R. S. Brush, and R. E. Anderson. 2005. Detailed characterization of the lipid composition of detergent-resistant membranes from photoreceptor rod outer segment membranes. *Invest. Ophthalmol. Vis. Sci.* **46:** 1147–1154.
29. Fliesler, S. J., and R. E. Anderson. 1983. Chemistry and metabolism of lipids in the vertebrate retina. *Prog. Lipid Res.* **22:** 79–131.
30. Niu, S. L., D. C. Mitchell, S. Y. Lim, Z. M. Wen, H. Y. Kim, N. Salem, Jr., and B. J. Litman. 2004. Reduced G protein-coupled signaling efficiency in retinal rod outer segments in response to n-3 fatty acid deficiency. *J. Biol. Chem.* **279:** 31098–31104.
31. Bloch, K. 1983. Sterol structure and membrane function. *CRC Crit. Rev. Biochem.* **14:** 47–92.
32. Yeagle, P. L. 1993. The biophysics and cell biology of cholesterol: a hypothesis for the essential role of cholesterol in mammalian cells. *In* Cholesterol in Membrane Models. L. Finegold, editor. CRC Press, Boca Raton, FL. 1–12.
33. Serfis, A. B., S. Brancato, and S. J. Fliesler. 2001. Comparative behavior of sterols in phosphatidylcholine-sterol monolayer films. *Biochim. Biophys. Acta.* **1511:** 341–348.
34. Berring, E. E., K. Borrenpohl, S. J. Fliesler, and A. B. Serfis. 2005. A comparison of the behavior of cholesterol and selected derivatives in mixed sterol-phospholipid Langmuir monolayers: a fluorescence microscopy study. *Chem. Phys. Lipids.* **136:** 1–12.

35. Mitchell, D. C., M. Straume, and B. J. Litman. 1992. Role of sn-1-saturated,sn-2-polyunsaturated phospholipids in control of membrane receptor conformational equilibrium: effects of cholesterol and acyl chain unsaturation on the metarhodopsin I in equilibrium with metarhodopsin II equilibrium. *Biochemistry.* **31:** 662–670.
36. Niu, S. L., D. C. Mitchell, and B. J. Litman. 2002. Manipulation of cholesterol levels in rod disk membranes by methyl-beta-cyclodextrin: effects on receptor activation. *J. Biol. Chem.* **277:** 20139–20145.
37. Albert, A. D., and K. Boesze-Battaglia. 2005. The role of cholesterol in rod outer segment membranes. *Prog. Lipid Res.* **44:** 99–124.
38. Niu, S. L., and D. C. Mitchell. 2005. Effect of packing density on rhodopsin stability and function in polyunsaturated membranes. *Biophys. J.* **89:** 1833–1840.
39. Fulton, A. B., R. M. Hansen, and O. Findl. 1995. The development of the rod photoresponse from dark-adapted rats. *Invest. Ophthalmol. Vis. Sci.* **36:** 1038–1045.
40. Vigh, L., H. Nakamoto, J. Landry, A. Gomez-Munoz, J. L. Harwood, and I. Horvath. 2007. Membrane regulation of the stress response from prokaryotic models to mammalian cells. *Ann. N. Y. Acad. Sci.* **1113:** 40–51.
41. Dratz, E. A., and L. L. Holte. 1992. The molecular spring model for the function of docosahexaenoic acid (22:6w3) in biological membranes. *In* Essential Fatty Acids and Eicosanoids: Invited Papers from the Third International Congress. A. Sinclair and R. Gibson, editors. American Oil Chemists' Society, Champaign, IL. 122–127.
42. Tulenko, T. N., K. Boeze-Battaglia, R. P. Mason, G. S. Tint, R. D. Steiner, W. E. Connor, and E. F. Labelle. 2006. A membrane defect in the pathogenesis of the Smith-Lemli-Opitz syndrome. *J. Lipid Res.* **47:** 134–143.